4-2009

Simulation and Behavior of Corrosion Deteriorated Reinforced Concrete Members

M. A. Shayanfar
Iran University of Science and Technology

Amir Safiey
Clemson University, asafiey@g.clemson.edu

SIMULATION AND BEHAVIOR OF CORROSION DETERIORATED REINFORCED CONCRETE MEMBERS

M. A. Shayanfar[1], A. Safiey[2]
[1]School of Civil Engineering., Iran University of Science and Technology, Tehran, Iran
[2]Moshanir Consultant Engineers, Park Prince Buildings, Tehran, Iran

ABSTRACT
Several reinforced concrete (RC) infrastructures are now crumbling from corrosion of steel bars in concrete. The paper presents the recent advancements in analytical simulation of corrosion aftereffects on behavior of RC members. The model juxtaposes the experimental findings with analytical relationships. The implementation of the model into a nonlinear finite element formulation as well as the experimental and analytical backgrounds are discussed. The abilities of the resulted program have been studied by modeling some experimental specimens showing a reasonable agreement between the analytical and experimental findings.

Keywords: reinforced concrete, corrosion, bond-slip, nonlinear finite element method, tension stiffening

1. INTRODUCTION
The integrity of many RC buildings and infrastructures are compromised due to some dangerous effects of the aggression of the corrosive agents. To evaluate the effects of these types of the damages on the total behavior of reinforced concrete structures, the nonlinear finite element models for reinforced concrete need an improvement to take the effects of corrosion of the steel bars into account. A survey on the literature reveals that there is a knowledge gap in this area of researches; relatively few studies addressed explicitly analytical modeling of corroded reinforcements in RC members. The amalgamation of the available analytical models is presented by Table 1. All of the reviewed models have their own advantages and disadvantages. Some of them sound to be more valuable from engineering point of view while the others seem to be more complicated and suitable at elemental level. The common point of these models is application of especial elements between concrete and reinforcement to represent the bond-slip behavior and associated damages as results of the corrosion of reinforcements.
Corrosion of steel reinforcements in the RC structures diminishes the total load bearing capacity of RC structures. This happens not only by means of depletion of rebar cross-sectional area, but also by bond deterioration as reported by some of the researchers, e.g. [6]. Tension-stiffening phenomenon in reinforced concrete is developed as a result of steel and concrete bond that occurs between the tensile cracks. Therefore, degrading effects of corrosion to the bond between steel and concrete could be taken into consideration more effectively by a proper tension

stiffening model. This would be a more practical method to solve the problem than utilization of link elements between steel bar and concrete. For this purpose at first step, a comprehensive experimental program including 58 cylindrical reinforced concrete specimens under various levels of corrosion is conducted. Some of the specimens (44) are located in large tub containing water and salt (5% salt solution). An electrical supplier has been utilized for the accelerated corrosion program. Afterwards, the tensile behavior of the specimens was studied by means of the direct tension tests. For each specimen, the tension-stiffening curve is studied at various load levels. Average crack spacing, loss of cross-section area due to corrosion, the concrete contribution to the tensile response for different strain levels, and maximum bond stress developed at each corrosion level are studied, and their appropriate relationships are proposed. Afterwards based on the experimental program and some analytical relationships, a new bond-slip-tension-stiffening model considering the effects of corrosion of reinforcement was developed. It is implemented into nonlinear finite element relationships as a part of a hypoelastic model of reinforced concrete. Finally, the performance of the program in handling nonlinear analysis of corroded reinforced concrete members is validated.

Table 1: Amalgamation of current literature

Researchers	Subject of simulation	Framework for constitutive relations	Corrosion and bond-slip representation
Coronelli and Gambarova [1]	RC beam	Incremental stress–strain relation for concrete, with smeared rotating cracks	Link element
Dekoster et al. [2]	RC beam	Elasto-plastic and damage Mechanics	Special link element called "rust"
Lundgren [3]	Direct tension test specimens	Theory of plasticity	Special layer of elements between steel and concrete
Lee et al. [4]	RC beam	Incremental stress–strain relation for concrete	Bond element
Amleh and Ghosh [5]	Direct tension test specimens	Elastic and plastic Model	Pressure–overclosure relationship

2. EXPERIMENTAL PROGRAM

A total of 58 specimens have been prepared for the experimental program. Specimens were divided into 7 types according to their sizes (see Table 2). From each type, 2 specimens (totally 14) were used as control and were not placed in the corrosive conditions. The rest of the specimens (totally 44) have been kept in the corrosive environment until the expected level of corrosion achieved. Subsequently, all of the specimens including non-corroded samples were tested by direct tension test on the embedded rod. Medium strength concrete (26 MPa) was used. The mean value of physical and mechanical properties of each type of rebars and concrete were measured (see [7] for details). Concrete cylinder specimens had a constant 500 mm length and variable diameter (60, 100, 150 mm). One deformed

steel reinforcement has been embedded in the middle of the concrete cylinder. This steel bar was extended adequately outside the two ends of the specimen. The specimen diameter and reinforcement diameter have been chosen in a manner to facilitate the feasible study of the effects of some important parameters such as clear concrete cover, ratio of clear concrete cover to rebar diameter, and ratio of rebar diameter to reinforcement ratio. For the construction of the specimens, 500 mm long rubber molds have been used. The molds have been set on a special chassis vertically. Steel reinforcement has been placed in the middle of the specimens to pass through the existing socket on an especial chassis at the end area. This set has been placed on a vibration table and the ready mixed concrete has been cast in mold layer by layer. After 24 hours, the molds have been opened and the specimens were cured in the ambient temperature for 28 days. The exposed parts of the reinforcement and the end areas of the RC specimens at the top and bottom surface were coated by epoxy. The extended steel bar outside the concrete was covered by two layers of tape, electrical tape followed by duct tape. The specimens have been immersed into a fiberglass tub containing a solution of water and salt (5%). An electric supplier has been utilized to subject the specimens to voltage of 24 V and current density of 8 A. The direction of the electric current was set so that the reinforcement served as the anode while the bare metal wire which was spread over the specimens served as cathode (see Figure 1). The duration of the accelerated corrosion procedure was estimated by Faraday's law to reach the required corrosion levels; with periods ranging from one day to one month. The actual values of degree of corrosion were calculated by breaking the specimens to retrieve the reinforcing bar after completion of the tests. The reinforcement bar for each specimen was cleaned and carefully scrubbed with a wire brush to assure that the bar was free from any adhering corrosion products. Special attention had been paid not to alter the base metal. The reinforcing bar was then carefully weighed to determine the actual corrosion degree.

Two special metal plates were fabricated, and each one was affixed to the top and the bottom of the specimens by three screws for measurement of specimen axial deformation. The LVDT (Linear Voltage Differential Transducer) system was employed to measure axial deformations. One gage was attached to the top plate and another one to the bottom plate for this purpose; the values of axial deformation of the specimen in each stage of loading were recorded by connecting them to the data logger apparatus. To measure reinforcing steel elongation, a displacement gage was affixed to the reinforcing bar at the top and another one at the bottom, connected to another LVDT system. The axial tensile forces were applied by a hydraulic jack and measured by a load cell connected to the top bracket. The axial load values were measured continuously by a data logger equipment (see Figure 2). The axial forces were increased to reach yielding capacity of the steel reinforcement; the tests were ceased by the onset of plastic deformations, and the number of transversal cracks and minimum and maximum crack spacing were recorded for each specimen. Eventually, actual degrees of the corrosion were measured for the corroded RC specimens as described earlier.

Figure 1. Accelerated corrosion program [7]

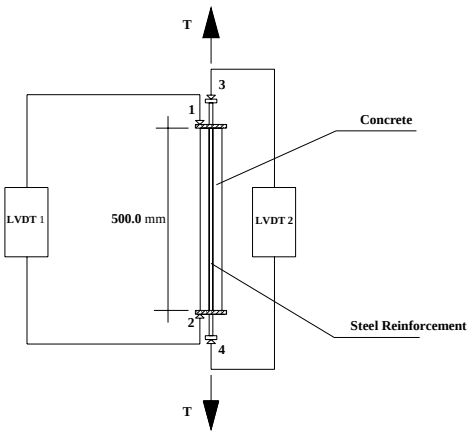

1: Displacement gage for speciemn at top
2: Displacement gage for speciemn at bottom
3: Displacement gage for bar at top
4: Displacement gage for bar at botttom

(a) Schematic representation **(b) Photo**

Figure 2. Details of the direct tension tests [7]

Table 2. The specimens overview [7]

Type	Specimen	c (mm)	ρ	c/d
1	S12-60	24	0.04	2.0
2	S12-100	44	0.0144	3.67
3	S18-60	21	0.09	1.167
4	S18-100	41	0.0324	2.278
5	S18-150	66	0.0144	3.67
6	S25-100	37.5	0.0625	1.5
7	S25-150	62.5	0.0278	2.5

The Corrosion levels, ultimate crack spacing, concrete stress contribution, bond strength, specimens' total applied tensile load versus average reinforcement strain and effect of corrosion on the cross-section area of the reinforcement are studied for specimens. The results of the experimental investigation reported elsewhere [7]. Some of the empirically obtained formulas are summarized by Table 3.

Table 3: Review of some proposed relationships [7]

Parameter	Formula
Average Final Crack Spacing	$S_m = 2.35c.\begin{cases}1 & C_w = 0\\ 1.533 - 0.3\,\frac{c}{d_0} + 4.2(\frac{C_w.d_0}{9c})^2 & C_w > 0\end{cases}$
Steel reinforcement yield strain	$\varepsilon_y = \frac{f_y}{E_s}.\begin{cases}1 & C_w = 0\\ 0.907 - 0.757\,\frac{C_w d_0}{9c} + 0.0087\,\frac{c}{d_0} & C_w > 0\end{cases}$
Reinforcement cross-sectional area	$A_s = A_{s0}.\begin{cases}1 & C_w = 0\\ 1.2 - 0.35\frac{C_w d_0}{9c} - 0.08\frac{c}{d_0} & C_w > 0\end{cases}$
Ultimate bond strength	$f_{bu} = \frac{0.4c}{d_0}\sqrt{f_c}$

3. MODELING STRATEGIES

In tension, the model adopts a macroscopic approach that is directly integrated into the concrete law. It simulates implicitly the reinforcing bar-concrete interaction using tension-stiffening factors adjustable according to the nature of specimen that vary as a function of the member strain, clear concrete cover, bond-slip behavior, degree of steel bar corrosion and amount of steel reinforcements. The tension-stiffening curve consists of two distinct states, namely “multiple cracking state” and “final cracking state.” Therefore, the uniaxial tensile stress-strain curve of a RC element could be divided into three states (see Figure 3-a): (a) “uncracked state” (path OA), (b) “multiple cracking state” (path AB) and (c) “final cracking state” (path BC). The numerical strategy of the proposed model is to discretize the tensile stress-strain curve by a set of discrete points called “principal points.” Those are connected by straight line to form a polygon similar to Figure 3-b. The number of “principal points”, N, is a constant value for a specific RC element during each analysis. This value probably differs from a RC element to another, depending on its characteristics; the minimum value of N is 4; because at least for describing the reinforced concrete tensile stress-strain curve, three lines are necessary. The computed stress and strain values corresponding to “principal points” are stored in two separate vectors, namely: $\{esm\}$ and $\{scm\}$; the dimensions of these two vectors are equal to the number of “principal points,” N. The value of tensile stress corresponding to the specific tensile strain could be

calculated by a linear interpolation. This concept and a sample for interpolation between the "principal points" are represented in Figure 3-b. For $i=1$, the values $esm(i=1)$ and $scm(i=1)$ are equal to zero. When $i=2$, the values $esm(i=2)$ and $scm(i=2)$ are equal to ε'_{cr} and f'_t; when i exceeds 2 the "multiple cracking state" is started and this state lasts until the value of a becomes less than $0.5S_m$. The values of stress and strain corresponding to the "principal points" in "multiple cracking state" is calculated by the following formulas:

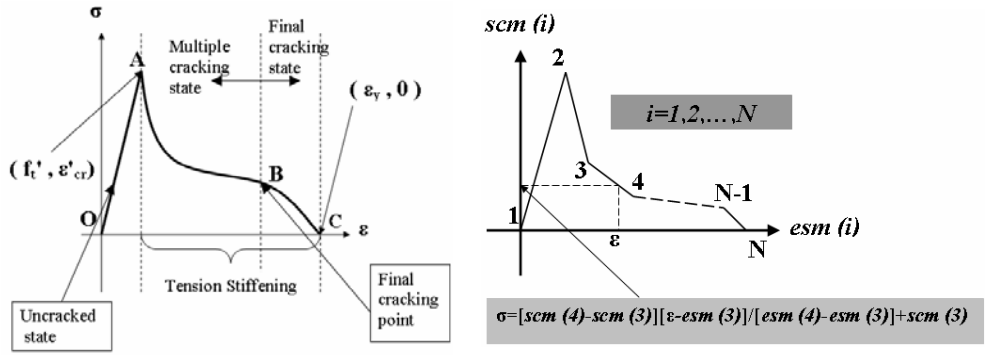

(a) Schematic representation of tension stiffening curve

(b) Idealization of RC tensile behavior and a sample for linear interpolation between principal points

Figure 3. Tension-stiffening [8]

$$esm(2<i<N-1)=\left(\frac{1+n\rho}{n\rho}\frac{\cosh(ka)}{\cosh(ka)-1}-\frac{\sqrt{1+.5\cosh(2ka)-\dfrac{.75\sinh(2ka)}{ka}}}{(\cosh(ka)-1)n\rho}\right).\left(\varepsilon'_{cr}(\exp(-550.esm(i)-\varepsilon'_{cr}))\right) \quad (1)$$

$$scm(2<i<N-1)=\left(\frac{\sqrt{1+.5\cosh(2ka)-\dfrac{.75\sinh(2ka)}{ka}}}{\cosh(ka)-1}\right)\left(f'_t(\exp(-550esm(i)-\varepsilon'_{cr}))\right) \quad (2)$$

The derivation processes of above equations are presented in [8]. Parameter a is the half of the spacing between the two faces of two adjacent cracks in a tensile member. The value of $2a$ for the first "principal point" of "multiple cracking state" ($i=3$) is equal to element length perpendicular to crack direction, *L*. For the second point of "multiple cracking state", $i=4$, the value of parameter $2a$ is bisected and it gets the value of $L/2$. For the next points this procedure will be continued until a becomes less than half of the average final crack spacing (S_m); at this point ($i=N-1$) which is called "final cracking point," the "multiple

cracking" curve is completed. At "final cracking state," the curve corresponding to this part is idealized by a line which is defined by two points, namely, "final cracking point" ($i = N - 1$) and "ultimate tensile point" ($i = N$). At this stage, $\{esm\}$ and $\{scm\}$ vectors are computed by these two formulas:

$$esm(i = N - 1) = \varepsilon_y - \frac{f_{bu}\Psi.S_m}{A_s E_s.2\sqrt{3}} \tag{3}$$

$$scm(i = N - 1) = 0.577\, f_t' \exp(-550(esm(i) - \varepsilon_{cr}')) \tag{4}$$

For simplicity and due to the lack of information about corrosion effect on "final cracking state," the "final cracking state" is neglected for corroded RC elements, therefore, Eqs. (3) and (4) change to:

$$esm(i = N - 1) = \varepsilon_y \quad , \quad scm(i = N - 1) = 0 \tag{5}$$

and the "final tensile point" is calculated by:

$$esm(i = N) = \varepsilon_y \quad , \quad scm(i = N) = 0 \tag{6}$$

A comparison between Eqs. (5) and (6) shows that the elements $i = N - 1$ and N has the same values for the corroded RC elements, leading to removal of the "final cracking state."

4. APPLICATION

The proposed tension-stiffening model is implemented into a nonlinear finite element analysis program which is called HODA. In this section, the abilities of the developed program on the analysis of field corroded RC beam specimens are verified.

The history, capabilities, element library, constitutive models and limitations of HODA nonlinear finite element analysis program used in this study are discussed elsewhere [9]. This program can depict, through the entire monotonically increasing load range, the static and reversed cyclic response of any plain, reinforced or prestressed concrete structures that is composed of thin plate members. This includes beams, slabs (plates), shells, folded plates, box girder, shear walls, or any combination of these structural elements. Time-dependent effects such as creep and shrinkage can be also studied. The element library includes membrane, plate bending, facet shell, one-dimensional bar, and boundary elements. The facet element has been used for modeling the RC beams. The program employs a layered finite element approach. The structure is idealized as an assemblage of thin constant thickness plate elements with each element subdivided into a number of imaginary layers. Each layer is assumed to be in plane stress

condition, and can be in any state - uncracked, partially cracked, fully cracked, non-yielded, yielded, and crushed- depending on the stress or strain conditions. Analysis is performed using an incremental-iterative tangent stiffness approach, and the stiffness of the element is obtained by adding the stiffness contributions of all layers at each Gauss quadrature point. Appropriate convergence/divergence criteria are utilized to stop the iterations in each load step as soon as a required degree of accuracy has been attained. Concrete are assumed to be as a stress-induced orthotropic material. The hypoelasticity constitutive relationship developed by Shayanfar has been used for modeling of the uncracked concrete. Smeared crack approach has been adopted for modeling of the cracked concrete. Thorenfeldt, et al. relationship which is able to accurately represent the family of stress-strain curves for different strength concretes including the high strength concrete is employed. In this research, the program has been modified to include tension-stiffening effect considering bond-slip and corrosion effects in reinforced concrete structures. The steel reinforcement is treated in HODA program as an elasto-plastic-strain-hardening material. A slightly modified form of the biaxial strength envelope curve developed by Kupfer, et al. is used in the program built up in the present study [9 and 10].

Three reinforced rectangular beams with f_c' equal to 70.1 MPa –that are almost high strength type concrete- were tested by Lee, et al [4]. Three beam specimens of their tests, namely BCD1, BCD2 and BCD3 are investigated in this study. The beams were 250x200 mm^2 in cross-section and they were supported over a clear span of 2000 mm (see Figure 4). It was subjected to two concentrated loads. The details of the reinforcement layout and the geometry of the beams are shown in Figure 4. The material properties of the concrete and the steel reinforcement are given in Table 4. The rate of reinforcement corrosion of each specimen is available on Table 5. Because of symmetry of load and geometry of the beams, only one-half of the beams are modeled in the finite element idealization. The beam specimen is discretized into 120 facet shell elements as illustrated in Figure 4. Plane stress conditions are assumed, therefore only one layer of concrete is sufficient. The longitudinal reinforcements are modeled using discrete bar elements without any flexural stiffness and are lumped in single bars at the reference surfaces. A 4x4 Gauss quadrature is used for estimating the integrations involved. The vertical loads are applied in 30 load steps with smaller increments of loads being applied just before the beam reaches its ultimate load stage. It would improve the rate of convergence of the solution and the accuracy in predicting the failure load. The smeared fixed crack model is used for crack modeling. All of the elements classified into two groups according to their tensile behavior; first group consists of reinforced elements with “tension-stiffening” behavior according to the proposed model; second group, consists of elements without reinforcement and their tensile stress-strain curves are described by linear “tension-softening” behavior. The first group ultimate tensile strain is equal to reinforcement yielding strain, while for the second group, it was chosen near to the strain calculated by a simple formula proposed by Shayanfar et al. [11]; this formula defines the RC element ultimate

tensile strain as function of element size in a very simple manner. This is used to remedy mesh size dependency in a nonlinear finite element formulation for reinforced concrete structures.

The analytical and experimental load-deflection curves for the beams BCD1 to BCD3 are plotted in Figure 5. The analytical results are a little bit stiffer than the experimental results and in good agreement with experimental findings. The stiffer response of model can be related to non-uniform corrosion, pitting, and longitudinal cracking due to rebar corrosion and the other items that arise from haphazard nature of corrosion and cracking phenomenon in RC members.

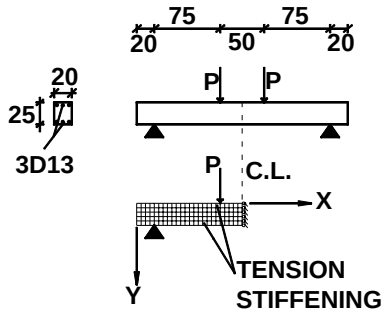

1. ALL DIMENSIONS ARE IN *cm*.
2. CONCRETE COVER IS 3 *cm*.

Figure 4. BCD1, BCD2 and BCD3 experimental details and finite element idealization

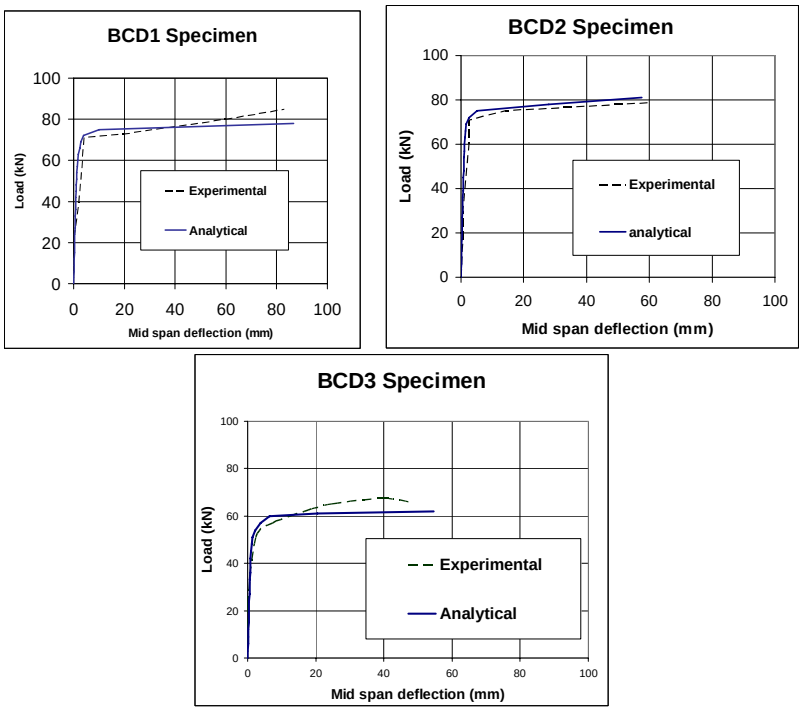

Figure 5. Experimental and analytical comparison

Table 4: Material properties of RC beams

Properties	Beams
$A_s(mm^2)$	256.46
$f_c(MPa)$	70.1
$E_0(MPa)$	38500
ε_c	0.002
ε_{cu}	.004 (Assumed value)
$f_t'(MPa)$	3.67
$f_y(MPa)$	359.4
$E_s(MPa)$	197000
$E_s^*(MPa)$	1300 (Assumed value)
ε_{su}	0.15
$E_b(MPa/mm)$	450 (Assumed value)

Table 5. Rate of corrosion in RC beams

Beams	$C_w(\%)$
BCD1	3.8
BCD2	7.9
BCD3	25.3

5. CONCLUSION AND SUMMARIES

The conclusions drawn from experimental investigation, which is presented with more details in [7], could be summarized as follows: The tensile behavior of reinforced concrete considering corrosion effects was studied experimentally. The specimen properties were chosen in a manner to reflect the effects of the governing parameters in the tensile behavior of the reinforced concrete specimens. The following conclusions are drawn:

1. (a) The ultimate crack spacing for non-corroded specimens mainly is related to the clear concrete cover of specimens. (b) This length will be increased for corroded specimens by increasing the degree of corrosion and appearance of longitudinal cracks. (c) This is merely related to the decline of the bond between concrete and steel reinforcement demanding for greater length to transfer tensile forces from the steel to the concrete.
2. The study of the specimens concrete stress contribution versus steel reinforcement average strain reveals that the tension stiffening of reinforced concrete is very sensitive to the degree of reinforcement corrosion. Severe corrosion results in bond breakdown between concrete and steel reinforcement; nearby no contribution of the concrete in the tensile response

beyond cracking (tension cut-off) could be expected for specimens in such condition. The lower levels of the reinforcement corrosion have considerable impacts on the stiffness and the ultimate strain of the tension-stiffening curve. The ultimate tensile strain of these curves for non-corroded specimens is close to the reinforcement yielding strain, but it will be reduced nearby to the strain corresponding to the tensile strength of concrete by increasing the levels of corrosion. The study on total applied tensile forces versus the average reinforcement strain curves also shows that the corrosion will decrease concrete stress contribution in cracking states.

3. The study of ultimate average bond strength deterioration of specimens and loss of cross-section area of reinforcement as result of corrosion reveals that the ratio of clear concrete cover to the size of the reinforcement has an important role in controlling these two important effects of corrosion.
4. Some empirical formulas for prediction of some of the studied parameters (e.g. ultimate crack spacing) were proposed and compared with the experimental findings of a similar program. Acceptable correlations were observed between the results of these two research programs.

Moreover, a new semi-analytical model describing the tension-stiffening phenomena considering bond-slip behavior and corrosion is represented; see also [8]. The model splits the tension-stiffening curve into two states, namely: “multiple cracking state” and “final cracking state.” The proposed procedure predicts the “final cracking point” by an experimental criterion by setting a lower bound for the average final crack spacing parameter. Another novel aspect of the tension-stiffening model is the discretization of the tension-stiffening curve by a set of points called “principal points” and using linear interpolation technique for computing tensile stress corresponding to a specific tensile strain. This model has been implemented into the HODA program. This program utilizes the hypoelastic model and the smeared crack approach. The model has been tested by means of analyzing three field RC beams; the RC beams have the same geometry and material property but different rates of tensile rebar corrosion. The analytical responses using HODA program reveals good agreements with the experimental findings. The principal features of this paper in a quick view are:

1. Without using any special element between concrete and steel by only modifying the tension-stiffening curve depending on the rate of steel bar corrosion, the corroded RC elements can be modeled with a reasonable accuracy. This method is applicable for a vast variety of steel reinforcement corrosion rates.
2. A new bond-slip-tension-stiffening algorithm has been introduced.
3. Ductility and the failure points of the corroded reinforcements RC members have been predicted reasonably by the means of a simple nonlinear finite element model.

REFERENCES

1. Coronelli, D. and Gambarova, P. (2004), “Structural assessment of corroded reinforced concrete beams: Modeling Guidelines”, *J. of Str. Eng., ASCE,*

130(8), 1214-1224.

2. Dekoster, M., Buyle-Bodin, F., Maurel, O. and Delmas, Y. (2003), "Modeling of the flexural behavior of RC beams subjected to localized and uniform corrosion", *Eng. Str.*, **25**, 1333-1341.
3. Lundgren, K. (2001), "Bond between corroded reinforcement and concrete", Report No.00:3, Department of Structural Engineering, Chalmers University of Technology, Gotenberg, Sweden.
4. Lee, H.S., Noguchi T., and Tomosawa F. (2000), "Analytical evaluation of structural performance of reinforced concrete beams considering degree of reinforcing bar corrosion", *Proceedings of Fourth International Conference on Repair, Rehabilitation and Maintenance of Concrete Structures and Innovations in design and Construction, Seoul, Korea*, **SP 193-46**, 779-789.
5. Amleh L., and Ghosh A. (2006), "Modeling the effect of corrosion on bond strength at the steel–concrete interface with finite-element analysis", *Can. J. Civ. Eng*. 33: 673–682.
6. Amleh, L., and Mirza, M.S. (1999), "Corrosion influence on bond between steel and concrete", ACI Str. J., 96(3), 415-423.
7. Shayanfar, M. A., Ghalehnovi, M., and Safiey, A., "Corrosion effects on tension stiffening behavior of reinforced concrete," *Computers and Concrete: An International Journal*, Vol.4, No.5, pp.403-424, 2007.
8. Shayanfar, M. A., and Safiey, A., "A new approach for nonlinear finite element analysis of reinforced concrete structures with corroded reinforcements," *Computers and Concrete: An International Journal*, Vol. 5, No. 2, pp. 155-174, 2008.
9. Shayanfar, M. A. (1995), "Nonlinear finite element analysis of normal and high strength concrete structures", PhD thesis, McGill University, Montreal, Canada.
10. Shayanfar, M. A., and Safiey, A., "Hypoelastic modeling of reinforced concrete walls," *Computers and Concrete: An International Journal*, Vol. 5, No. 3, in press, 2008.
11. Shayanfar, M.A., Kheyroddin, A., and Mirza, M.S. (1997), "Element size effects in nonlinear analysis of reinforced concrete members", Com. & Str., 62(2), 339-352.